symmetry

MDPI

Article

Chiral Separation of Vildagliptin by Capillary Electrophoresis—The Study of Enantiomeric Complexation

Lajos Attila Papp [1], Gabriel Hancu [1,*], Zoltán István Szabó [2,3], Blanka Székely-Szentmiklósi [1], Tamás Gáti [4], Béla Fiser [5,6,7], Márta Kraszni [8] and Gergő Tóth [8]

1 Department of Pharmaceutical Chemistry, Faculty of Pharmacy, "George Emil Palade" University of Medicine, Pharmacy, Science and Technology Târgu Mureș, 540120 Târgu Mureș, Romania; lajos.papp@umfst.ro (L.A.P.); blanka.szekely-szentmiklosi@umfst.ro (B.S.-S.)
2 Department of Drugs Industry and Pharmaceutical Management, Faculty of Pharmacy, "George Emil Palade" University of Medicine, Pharmacy, Science and Technology Târgu Mureș, 540120 Târgu Mureș, Romania; zoltan.szabo@umfst.ro
3 Sz-Imfidum, Ltd., Str. Lunga nr. 504, 525401 Târgu Mureș, Romania
4 Servier Research Institute of Medicinal Chemistry (SRIMC), H-1031 Budapest, Hungary; tamas.gati@servier.com
5 Higher Education and Industrial Cooperation Centre, University of Miskolc, H-3515 Miskolc, Hungary; bela.fiser@uni-miskolc.hu
6 Department of Biology and Chemistry, Ferenc Rakoczi II Transcarpathian Hungarian College of Higher Education, Transcarpathia, 90200 Beregszasz, Ukraine
7 Department of Physical Chemistry, Faculty of Chemistry, University of Lodz, 90-149 Łódź, Poland
8 Department of Pharmaceutical Chemistry, Semmelweis University, 1092 Budapest, Hungary; kraszni.marta@semmelweis.hu (M.K.); toth.gergo@pharma.semmelweis-univ.hu (G.T.)
* Correspondence: gabriel.hancu@umfst.ro

Abstract: Vildagliptin (VIL) is a dipeptidyl peptidase-4 inhibitor used in the treatment of type 2 diabetes mellitus; in therapy, it is available as the enantiomerically pure *S*-VIL, the other enantiomer *R*-VIL being considered as an enantiomeric impurity. A systematic screening of 16 cyclodextrin (CD) derivatives as chiral selectors was performed at three pH levels using phosphate (pH 2.5, pH 7.0) and acetate (pH 4.5) buffers. Method optimization employed an experimental design approach, systematically investigating the effect of buffer and CD concentration, buffer pH, capillary temperature, and applied voltage on the chiral resolution and analysis time. The method's analytical performance was thoroughly assessed and subsequently employed for determining the enantiomeric purity of VIL in a pharmaceutical formulation. The properties of the inclusion complexes, such as stoichiometry and atomic level intermolecular host–guest interactions were studied by NMR measurements and molecular modeling. Native α-CD at acidic pH has demonstrated its exceptional suitability for the separation of VIL enantiomers with a favorable migration order (*R*-VIL followed by *S*-VIL). The optimized analytical conditions (75 mM acetate buffer, pH 4.5, containing 50 mM α-CD, 18 kV applied voltage, and 15 °C capillary temperature) provided a baseline separation of VIL enantiomers within 9 min. The developed method represents a cost-effective alternative to the enantiomeric impurity control of VIL. Symmetry is often a fundamental aspect of molecular structures and interactions, and our detailed analysis of the chiral recognition process contributes to the understanding of symmetry-related aspects in molecular systems. This developed method not only offers a cost-effective alternative for the enantiomeric impurity control of VIL but also provides valuable information regarding the mechanism of the chiral recognition process, aligning with the broader themes of symmetry in molecular sciences.

Keywords: vildagliptin; chiral separation; capillary electrophoresis; enantiomeric purity; cyclodextrins; complexation mechanism

Citation: Papp, L.A.; Hancu, G.; Szabó, Z.I.; Székely-Szentmiklósi, B.; Gáti, T.; Fiser, B.; Kraszni, M.; Tóth, G. Chiral Separation of Vildagliptin by Capillary Electrophoresis—The Study of Enantiomeric Complexation. *Symmetry* **2024**, *16*, 17. https://doi.org/10.3390/sym16010017

Academic Editor: György Keglevich

Received: 29 November 2023
Revised: 14 December 2023
Accepted: 18 December 2023
Published: 22 December 2023

1. Introduction

Vildagliptin (VIL) is a dipeptidyl peptidase-4 (DPP-4) inhibitor used in the treatment of type 2 diabetes mellitus, a chronic condition in which the body does not properly use insulin, leading to high blood sugar levels. By inhibiting the DPP-4 enzyme, the metabolism of the two incretin hormones (glucagon-like peptide-1 and glucose-dependent insulinotropic polypeptide) is reduced, leading to an increase in insulin and a decrease in glucagon secretion under hyperglycemic conditions [1,2].

VIL has one chiral center in its structure (Figure 1), meaning it exists in two enantiomeric forms, and it is used in the therapy as an enantiomerically pure *S*-VIL; therefore, adequate analytical procedures are needed for the monitorization of its enantiomeric purity [3].

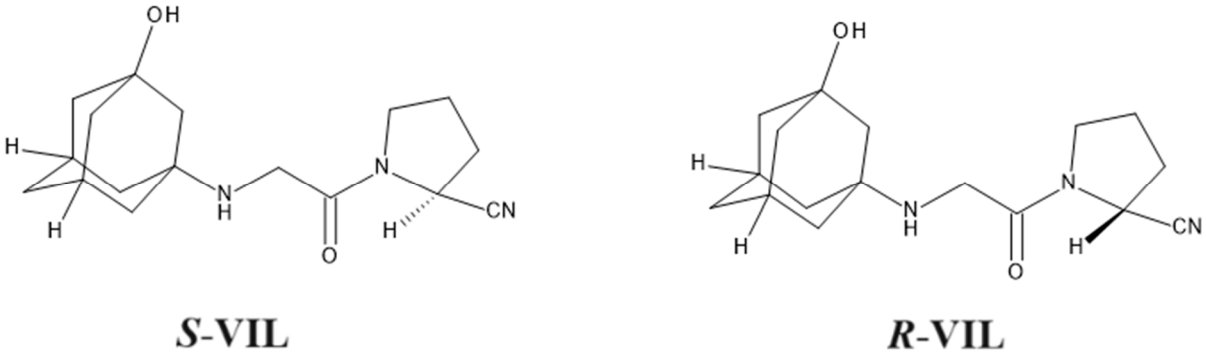

Figure 1. Chemical structure of VIL enantiomers.

Capillary electrophoresis (CE) is an attractive and viable alternative to high-performance liquid chromatography (HPLC), which is considered the "golden" standard technique in the field of chiral analysis. CE is characterized by having a low sample, chiral selector, organic solvent consumption, rapid method development, and short analysis time. Usually, in CE, a direct separation mechanism is applied by adding the chiral selector (CS) in the background electrolyte (BGE). Moreover, chiral CE methods offer inherent advantages due to the specific chiral separation mechanism, which can include a thermodynamic mechanism (difference in the stability of the CS-enantiomer complexes) and an electrophoretic mechanism (difference in the mobility of the same complexes) [4,5].

Cyclodextrins (CDs) are the most frequently employed CSs in CE. CDs are oligosaccharides consisting of 6, 7, or 8 D-glucopyranose units for α-, β-, and γ-CD, respectively, which form a cone-shaped cavity. A large variety of different native and derivatized, neutral, and ionized CDs were used successfully for the enantioseparation of a broad spectrum of pharmaceuticals. The UV transparency, good solubility, stability in the aqueous medium over a wide pH range, and the commercial availability of CDs contribute to their popularity as CSs in CE. Moreover, the possibility to perform a CS screening using different CD derivatives at different pH aids method development and ensures a high probability of successful chiral separation [6,7].

The chiral recognition mechanism of CDs generally involves the formation of inclusion complexes and secondary interactions, such as hydrogen bonds and dipole–dipole interactions, as well as ionic interactions (ionizable CDs) [8,9]. However, the formation of external-type complexes has also been described in some cases [10,11].

A CE method has been reported by Kazsoki et al. for the chiral separation of VIL employing sulfobutyl-ether-α-cyclodextrin (SBE-α-CD) as a CS in an acidic BGE (Tris-acetate buffer, pH = 4.75). The method underwent optimization using an orthogonal design. However, further adjustments to the conditions were necessary to improve peak shapes and increase the separation between the second migrating enantiomer and EOF [12]. Furthermore, a more cost-effective and widely available CD could potentially be employed for this purpose. Two chromatographic methods can also be found in the literature for the chiral analysis of VIL. An HPLC method capable of determining *R*-

VIL as a chiral impurity in the presence of the eutomer was reported by Srinivas et al. Cellulose-[tris(3,5-dimethylphenylcarbamate)]-based chiral column in combination with a mobile phase consisting of 20 mM borax buffer (pH 9.0)/acetonitrile/0.1% triethylamine (50:50:0.1, *v*/*v*/*v*) was employed [13]. Recently, our group published a reversed-phase HPLC method for the simultaneous quantification of *R*-VIL and four other organic impurities of VIL using a cellulose-based chiral stationary phase and a mobile phase consisting of methanol/water/diethylamine (80:20:0.2, *v*/*v*/*v*) [14].

The aim of our study was the development and validation of a CE method using CD as CS for the enantiomeric purity analysis of VIL, as well as the study of the complexation mechanism between the CS and VIL enantiomers by NMR spectroscopy and molecular modeling. As for the correlation with the symmetry concept, the inherent symmetry in molecular structures, particularly in the context of chiral recognition, is implicit in the discussion. The mention of inclusion complexes and various interactions contributing to chiral recognition aligns with the principles of symmetry in molecular systems.

2. Materials and Methods

2.1. Reagents and Samples

R-VIL and *R*,*S*-VIL were obtained from Pharmaffilities (Panchkula, Haryana, India). Phosphoric acid (85%), disodium hydrogen phosphate, sodium dihydrogen phosphate, sodium acetate, methanol, sodium hydroxide, and hydrochloric acid 37% were purchased from Merck (Darmstadt, Germany). Deuterium oxide (99.96% D) was obtained from VWR Chemicals (Belgium, Leuven). Ultrapure water was prepared by using a Milli-Q Direct 8 Millipore system (Milford, MA, USA).

Sixteen CDs from four different classes were used as potential CS, as follows: native (α-, β-, and γ-CD), derivatized neutral (2-hydroxypropyl-β-CD—2-HP-β-CD; 2-hydroxyethyl-β-CD—2-HE-β-CD, heptakis(2,6-di-O-methyl)-β-CD—DIMEB, heptakis(2,3,6-tri-O-methyl)-β-CD—TRIMEB, methyl-β-CD—M-β-CD), derivatized anionic (sulfobuthylether-β-CD—SBE-β-CD, carboxymethyl-β-CD—CM-β-CD, sulfated-β–CD—S-β-CD, succinyl-β–CD—Su-β-CD), single isomer anionic (octakis(2,3-di-O-methyl-6-sulfo)-γ-CD sodium salt, heptakis(2,3-di-O-methyl-6-sulfo)-β-CD sodium salt, heptakis(2,3-di-O-acetyl-6-sulfo)-β-CD sodium salt, hexakis(2,3-di-O-methyl-6-sulfo)-α-CD sodium salt). All CDs were obtained from Cyclolab R&D, Ltd. (Budapest, Hungary).

A placebo mixture of excipients identic with the composition of the analyzed pharmaceutical product (consisting of lactose, microcrystalline cellulose, sodium starch glycolate type A, and magnesium stearate) was kindly offered by a local pharmaceutical company. The drug product used for the application of the developed method (Agartha® (Gedeon Richter) 50 mg tablets) was purchased from a local pharmacy in Târgu Mures.

2.2. Instrumentation

Electrophoretic experiments were carried out on an Agilent 1600 CE system (Agilent Technologies, Waldbronn, Germany) equipped with a diode array (DAD) detector and Chemstation 7.01 software for data handling. Experiments were performed using an uncoated fused-silica capillary with 48 cm total, 40 cm effective length, and an internal diameter of 50 µm (Agilent, Germany).

Capillaries were conditioned by flushing with 1 M NaOH for 30 min, 0.1 M NaOH, and purified water for 20 min each. Between runs, the capillary was preconditioned by flushing with 0.1 M NaOH (2 min), water (1 min), and BGE (2 min).

The initial electrophoretic conditions were as follows: voltage 20 kV, capillary temperature 20 °C, UV detection at 205 nm, sample concentration 50 µg mL^{-1}, and hydrodynamic injection (50 mbar for 3 s).

The 1D ^{1}H NMR spectra for Job's plot were recorded with a Varian Mercury Plus spectrometer (400 MHz for ^{1}H) in D_2O. Then, 1D ^{13}C (deptqsp) and 2D ROESY (roesyph.2) experiments were performed using a Bruker Avance NEO 500 MHZ spectrometer equipped with TCI cryo probe head. Chemical shifts were referenced to internal methanol.

2.3. Preparation of Running Buffers and Solutions

BGE solutions were prepared by dissolving the appropriate amount of buffer constituents in ultrapure water and adjusting their pH, if necessary, with 1 M NaOH, 1 M phosphoric acid, (phosphate buffer), or 1 M hydrochloric acid (acetate buffer).

Additionally, 2 mg mL^{-1} stock solutions of *R*-VIL and *R*,*S*-VIL were prepared in methanol and then mixed and diluted with purified water to appropriate concentrations.

The commercial pharmaceutical product was analyzed by powdering ten tablets in a mortar and suspending an amount of powder equivalent to the medium weight of one tablet in 100 mL methanol and sonicating for 5 min. The suspension was centrifuged at 4000 rpm for 10 min using a Centurion K240 centrifuge (Centurion Scientific, Chichester, UK). The obtained supernatant was filtered through a 0.45 µm syringe filter and diluted with water to the appropriate concentration before use.

Both sample solutions and BGE were filtered through a 0.45 µm pore size membrane filter and degassed in an ultrasonic bath for 2 min before use. When not in use, all solutions were stored in the refrigerator.

2.4. Data Interpretation and Calculations

The obtained results were evaluated in terms of resolution (R_s) based on the $R_s = 2(t_2 - t_1)/(w_1 + w_2)$ equation, where the migration times (t_1 and t_2) and the peak widths (w_1 and w_2) were marked for the slow and fast migrating enantiomers, respectively.

Design Expert 7.0 statistical software (Stat-Ease, Minneapolis, MN, USA) was utilized for technique optimization in order to build the experimental plans and assess the results.

2.5. Molecular Modeling

The OPLS-AA force field [15], in combination with the Born implicit solvation model, was employed to optimize the 3D structure of α-CD and thus to achieve a suitable host for molecular docking. Both *S*-VIL and *R*-VIL were docked to the prepared α-CD using AutoDock Vina [16]. A grid box of 40 × 40 × 40 $Å^3$ was considered, and the exhaustiveness was set to 8 during the docking procedures. All in all, in each calculation, 9 binding modes were produced, and the corresponding binding affinities (E_A) were computed to select the best binding modes (lowest E_A). Additional complexes were prepared by reversing the orientation of the VIL enantiomers in the α-CD cavity. The selected and newly prepared complexes were further refined and optimized using the PM6 semi-empirical method [17]. To achieve the final structures and the corresponding thermodynamic properties, the Austin–Petersson–Frisch functional with dispersion (APFD) [18] in combination with 6–31 G(d) basis set was applied, and optimizations and frequency calculations were carried out. The Gaussian 16 program package was used to perform the quantum chemical computations. [19]. To mimic the effect of solvation, the CPCM implicit solvent model (water, ε = 78.3553) was employed as part of the quantum chemical calculations [20,21]. During the density functional theory calculations, both neutral and protonated VIL species were considered.

3. Results

3.1. Preliminary Experiments

Sixteen neutral and anionic CDs differing in cavity sizes, type, and substitution pattern (randomly substituted and single isomeric CDs) applied in the concentration range of 5–20 mM were screened at three pH levels (pH—2.5, 4.5, and 7.0). Given that VIL is a secondary amine exhibiting a distinct basic character (with a pK_a value around 9), it can be anticipated that the compound predominantly exists in its positively charged form within the investigated pH range, causing migration towards the cathode. The magnitude of electroosmotic flow (EOF), as a non-enantioselective driving force, can influence the migration times of analytes and can enhance or weaken the chiral separation. Under strongly acidic conditions, as in the case of BGE with pH—2.5, EOF is mainly suppressed, while at higher pH values, EOF increases with the increasing basicity of the BGE [22].

Consequently, for neutral CDs, screening was exclusively conducted in the positive polarity mode. In contrast, for anionic CDs, both normal and reversed-polarity experiments were undertaken. In strongly acidic conditions (pH—2.5), no chiral recognition was observed, while at pH 4.5, VIL enantiomers showed partial chiral resolution (*Rs* = 0.54) when applying α-CD as a CS. A partial chiral resolution was also achieved when using β-CD or DIMEB at pH 7.0 but with a lower chiral resolution. The enantiomeric migration order in all cases was favorable, with the distomer *R*-VIL migrating first, followed by the eutomer *S*-VIL. Based on the CS screening, α-CD was chosen as the CS for further investigations and method optimization. Representative electropherograms obtained during the screening phase are presented in Figure 2.

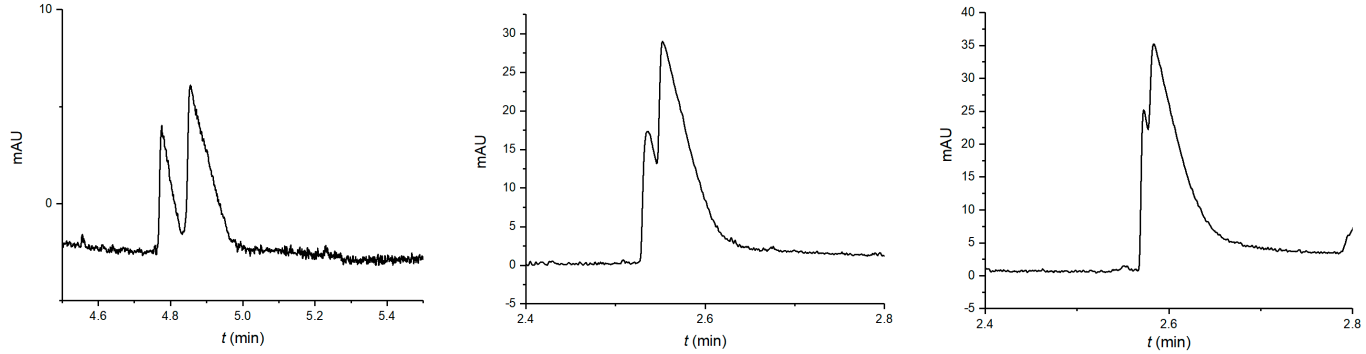

Figure 2. Chiral separation of VIL in the presence of (**a**) 20 mM α-CD, (**b**) 10 mM β-CD, (**c**) 20 mM DIMEB. Analytical conditions: (**a**)—50 mM acetate buffer (pH—4.5), (**b**,**c**)—5 mM phosphate buffer (pH—7.0) voltage: 20 kV, temperature: 20 °C, injection: 50 mbar/3 s.

3.2. Method Optimization

To determine the optimal analytical conditions, a multivariate approach was applied in two steps: first, a screening design, followed by an optimization design. Our aim was to develop a rapid and selective CE method capable of determining the enantiomeric impurity of VIL. Therefore, during method optimization, we chose to follow the chiral resolution and analysis time (represented by the migration time of *R*-VIL) as analytical responses. At first, a 2^{5-2} type fractional factorial screening design was applied to estimate factors with significant effects on the analytical responses. The five studied factors and their ranges were as follows: BGE pH of 4.5–5.5 (factor A), BGE concentration of 25–75 mM (factor B), α-CD concentration of 30–50 mM (factor C), capillary temperature of 15–25 °C (factor D), applied voltage of 15–25 kV (factor E). Each factor had a lower- and upper-level value, coded as −1 and 1. For the improved estimation of experimental error and to increase the number of degrees of freedom in the model, three additional injections were made at the center point of the experimental plan, with each factor set at the 0 level. The experimental matrix with the results obtained is presented in the Supporting Information Table S1. To evaluate the results, a simple first-order regression model was applied, and analysis of variance (ANOVA) was carried out to verify the significance of the model and its regression coefficients. One by one, the insignificant model terms were removed, and each time a term was removed, the mathematical model underwent another evaluation. The final regression equations for the resolution and analysis time were determined and are shown below in coded terms:

$$Rs = +0.96 + 0.35 * B - 0.19 * D - 0.19 * E \quad (1)$$

$$t = +5.43 + 1.70 * B - 2.55 * E - 1.63 * B * E \quad (2)$$

The BGE concentration and applied voltage were shown to have significant impacts on both experimental responses, while the capillary temperature proved to influence significantly only the resolution.

In the second step of method optimization, response surface methodology was carried out by applying a face-centered central composite design (FCCD) based on the results of the screening design. An experimental plan consisting of 20 experiments was constructed to evaluate the three selected variables, each being studied at three levels in the following ranges: BGE concentration of 60–90 mM (factor A), capillary temperature of 15–25 °C (factor B), and applied voltage: 15–25 kV (factor C). The rest of the factors, considered less significant, were held constant during the optimization (buffer pH—4.5 and 50 mM α-CD). The experimental matrix of FCCD with the results obtained are summarized in Supporting Information Table S1. The following final equations were obtained by ANOVA using a second-order polynomial model, which corresponds to the response surface methodology:

$$Rs = +1.47 - 0.068 * A - 0.31 * B - 0.31 * C + 0.070 * A * B - 0.095 * A * C + 0.058 * B * C - 0.14 * C^2 \quad (3)$$

$$t = +5.26 + 0.055 * A - 0.89 * B - 2.49 * C - 0.32 * A * C + 0.48 * B * C + 0.48 * C^2 \quad (4)$$

Table 1. Method validation data for the determination of *R*-VIL as a chiral impurity in S-VIL samples.

Precision		
Intra-day precision	migration time, RSD%	2.11
(c = 15 μg mL^{-1}, *n* = 6)	peak area, RSD%	1.45
Inter-day precision (c = 15 μg mL^{-1}, *n* = 18)	migration time, RSD%	2.64
	peak area, RSD%	1.87
Accuracy (recovery %)		
3 μg mL^{-1} (0.15%) (*n* = 6)	96.16 ± 3.07	
15 μg mL^{-1} (0.75%) (*n* = 6)	100.76 ± 1.28	
30 μg mL^{-1} (1.5%) (*n* = 6)	99.41 ± 2.13	
Linearity		
Regression equation (2–50 μg mL^{-1}) (0.1–2.5%)	y = 0.6242x − 0.3737	
Coefficient of determination	R^2 = 0.9964	
Sensitivity		
LOD (μg mL^{-1})	0.52	
LOQ (μg mL^{-1})	1.58	

The regression models proved to be significant, showing good performance indicators in terms of goodness of fit expressed by R^2 and R^2_{adj} and goodness of prediction expressed by Q^2 values, such as R^2 = 0.9671, R^2_{adj} = 0.9480, Q^2 = 0.8688 for the resolution, and R^2 = 0.9902, R^2_{adj} = 0.9857, Q^2 = 0.9613 for the analysis time, respectively.

As observed, both models contain quadratic and interaction terms, demonstrating the complexity of the effects of the studied experimental parameters on the responses. Based on the F values calculated for each model term during ANOVA, the capillary temperature (factor B) and the applied voltage (factor C) have relatively high and almost equal influences on the *Rs*-value. In the case of t, the applied voltage has the most prominent effect. The concentration of BGE (factor A) has the weakest influence on both responses, as expected. The three-dimensional response surface plots depicted in Figure 3 represent the interactions between two analytical parameters and their influence on the responses, while the third parameter is kept constant.

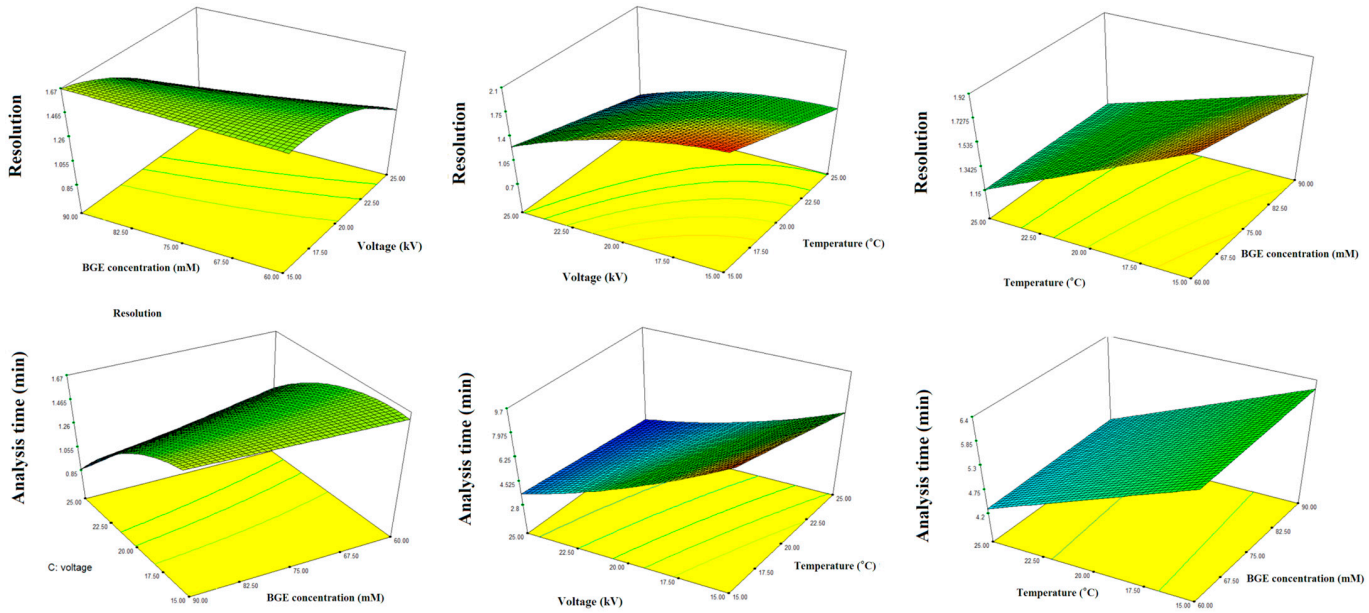

Figure 3. Three-dimensional response surface plots obtained for *Rs* and *t*.

The optimal parameter setting was established by using the optimization feature of the experimental design software. Maximizing *Rs* values and minimizing *t* were set as the objectives. The lower limits were set as 1.5 for *Rs* and 10 min for *t*, respectively. The factors were optimized with the same weight of priority. The optimal separation conditions were as follows: 75 mM acetate BGE, pH 4.5, 50 mM α-CD, 18 kV, 15 °C. Under the optimal analytical conditions, a baseline enantioresolution (*Rs* = 2.07) was achieved within 9 min. The generated current under these conditions was around 60 µA. A representative electropherogram of the separation of VIL enantiomers under optimized conditions is presented in Figure 4.

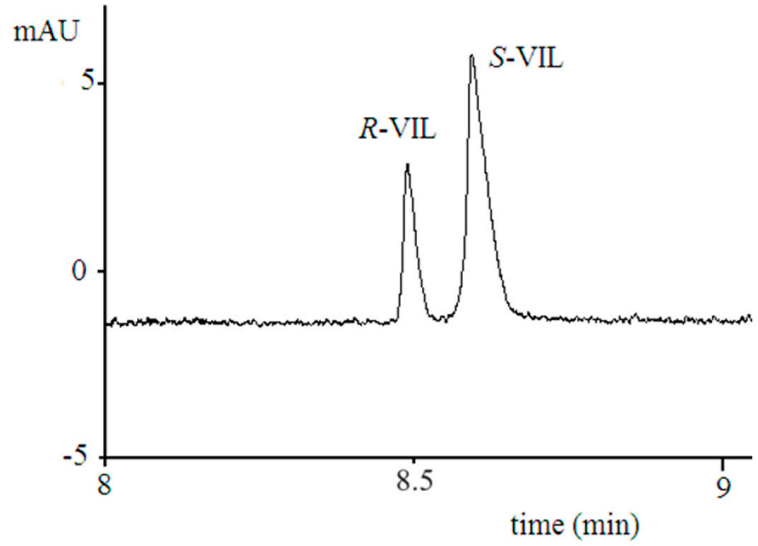

Figure 4. Enantiomeric separation of VIL under optimized conditions (75 mM acetate buffer, pH—4.5, containing 50 mM α-CD, 18 kV applied voltage, 15 °C capillary temperature, UV detection at 205 nm, injection: 50 mbar/3 s).

3.3. Method Validation

Our method was validated according to the International Council of Harmonization (ICH) guidelines, based on the specificity, precision, linearity, accuracy, limits of detection (LOD), and limit of quantification (LOQ) for the determination of *R*-VIL in VIL samples.

The specificity of the method was tested by spiking VIL enantiomers into the placebo mixture of the drug (excipients without VIL). There was no interference seen on the electropherograms with the excipients used in medication preparation. Precision (repeatability based on RSD% of migration time and peak area) and accuracy (calculated as recovery %) were estimated at three levels of the enantiomeric impurity, i.e., 0.15, 0.75, and 1.5% in the presence of 2000 μg mL^{-1} VIL.

The linearity of the method was investigated in the range of 2–50 μg mL^{-1} (0.1–2.5%) *R*-VIL in 2000 μg mL^{-1} VIL samples, performing three replicate injections at six concentration points. LOD and LOQ were calculated from signal/noise ratios 3:1 and 10:1, respectively. The LOQ of *R*-VIL was 1.58 μg mL^{-1}, corresponding to 0.079% impurity in 2000 μg mL^{-1} sample of eutomer, while LOD was 0.52 μg mL^{-1}, corresponding to 0.026% distomer. A representative electropherogram of VIL sample containing 0.1% *R*-VIL under optimal analytical conditions is presented in Figure 5.

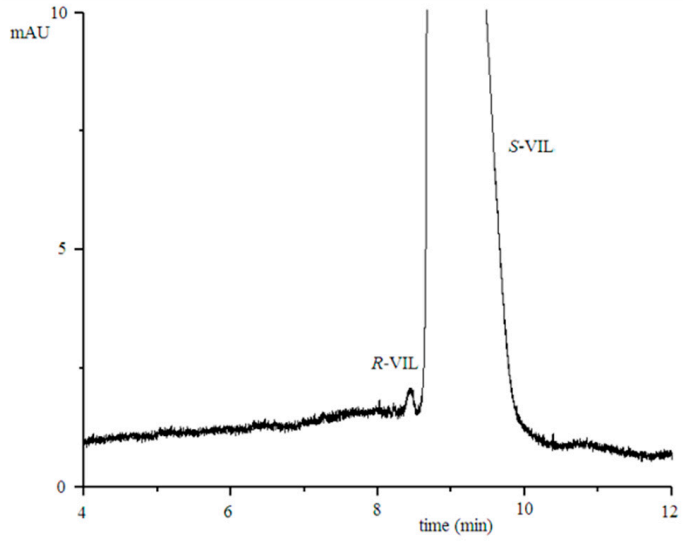

Figure 5. Determination of *R*-VIL in *S*-VIL sample. Sample containing 0.1% chiral impurity (experimental conditions the same as in Figure 4).

The validation data are summarized in Table 1. The RSD values of intra-day and inter-day precision were below 3%, and recovery values were above 95%.

According to the obtained results, our optimized method proved to be specific, precise, accurate, and linear for the determination of *R*-VIL as a chiral impurity in *S*-VIL samples.

The robustness of the method was verified by employing a Plackett–Burman design with 12 experiments by modifying the values of five experimental factors within the following ranges: applied voltage of 17–19 kV, capillary temperature of 14–16 °C, BGE concentration of 72–78 mM, BGE pH of 4.4–4.6, α-CD concentration of 48–52 mM. As analytical responses, the chiral resolution and migration time of both enantiomers were chosen. Statistical analysis (ANOVA) revealed no significant correlation between the studied factors and responses in the verified ranges, which demonstrates the robustness of this method.

The validated method was applied for the purity analysis of VIL tablets. The results showed that *R*-VIL could not be detected in the samples or was present in a concentration below the LOQ.

3.4. Characterization of Enantioselective Complexation

To describe the possible enantioselective interactions between α-CD and VIL enantiomers, NMR experiments and molecular modeling were performed.

The complexes' stoichiometry was quantified using the continuous variation method. Different cVIL/cCD ratios were used to measure the 1H NMR chemical shifts. However,

the total of cVIL + cCD remained constant at 30 mM. The chemical shift changes in certain hydrogens of VIL induced by the complexation and weighed by the molar fraction of VIL ($\Delta\delta \times x_{VIL}$) were plotted (Job's plot) as a function of the molar fraction of VIL (x_{VIL}). The registered Job's plot presented a maximum at 0.5 molar fraction plot indicating a 1:1 ratio of the host and guest in the complex (Figure 6a). The molecular geometry of the complex was investigated by two-dimensional phase-sensitive rotating frame nuclear Overhauser effect spectroscopy (2D ROESY) using 300 ms mixing time. In ROESY experiments, the samples contained 30 mM α-CD and 10 mM VIL. The 2D ROESY NMR spectrum of VIL and α-CD at 1:3 molar ratio showed the proximity of the H3 hydrogen of the host and several hydrogens of the guest molecules (Figure 6b), indicating that both the adamantane and pyrrolidine moieties of VIL may be involved in complex formation. Based on the 1D ^{1}H and ^{13}C (Supplementary Figures S1 and S2) spectra, we can assume that α-CD forms a complex with higher stability with the adamantane moiety. However, in the context of chiral recognition, the less stable inclusion with the pyrrolidine moiety may also play a role, given its proximity to the chiral center. In the ^{1}H NMR spectrum, chiral recognition is not observable because of the high degree of overlap of the multiple signals (Supplementary Figure S1). However, in the ^{13}C spectrum, *S*- and *R*-VIL signals are separated, indicating that the basis of the separation lies in the stability difference between the complexes of enantiomers with α-CD (Supplementary Figure S1).

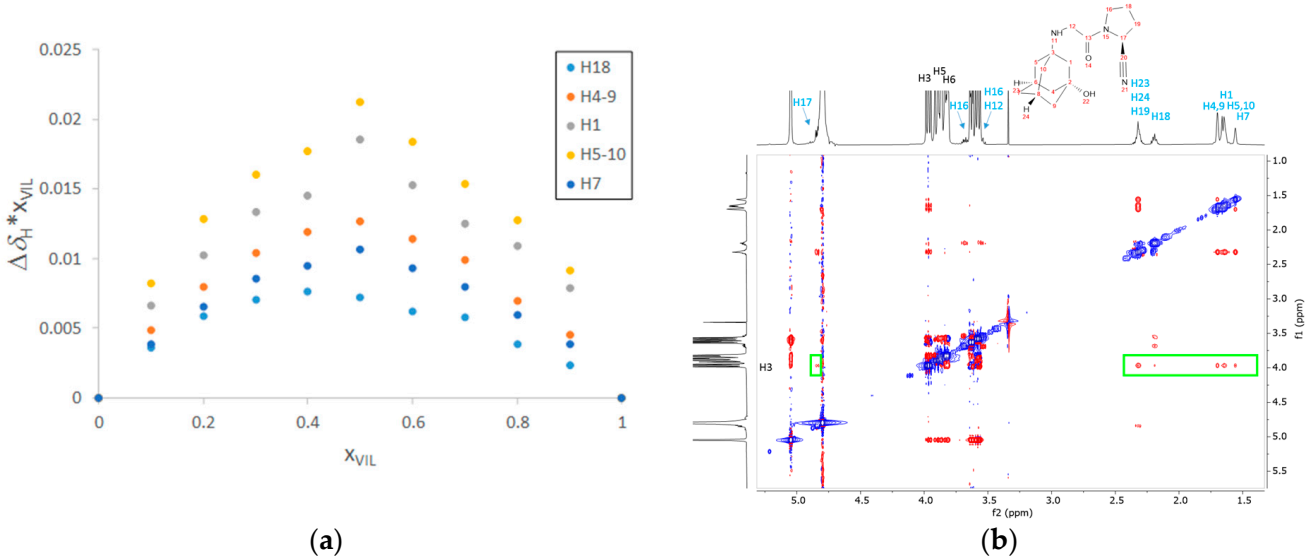

Figure 6. Job's plot (**a**) and 2D ROESY NMR spectrum (**b**) of the VIL—α-CD system.

The formation of VIL/α-CD inclusion complexes was verified by both molecular docking and quantum chemical calculations. The two possible types of inclusion complexes involving the adamantane- and the pyrrolidine moieties of VIL, respectively, are presented in Figure 7. Complex formation is thermodynamically favored for both *S*- and *R*-enantiomers. Furthermore, the preference towards the inclusion of the adamantane moiety of VIL into the cavity of the CD is also shown. In the case of the adamantane inclusion, by the protonation of VIL, the preference towards the *S*-VIL/α-CD complex further enhanced from −11.8 kJ/mol to −38.8 kJ/mol. These findings are in accordance with the experimentally observed migration order. To the best of our knowledge, the characterization of the VIL—α-CD complexes at the molecular level is reported for the first time.

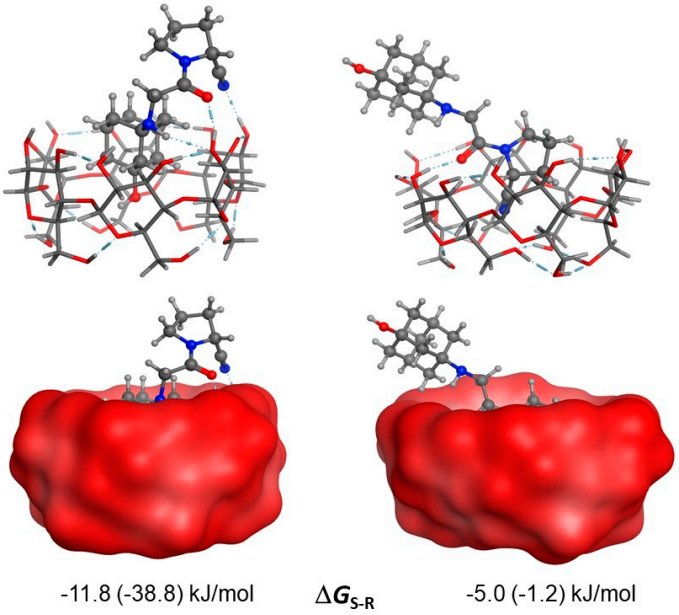

Figure 7. VIL/α-CD complexes along with the corresponding relative Gibbs free energies (DGS-R = GS–GR, in kJ/mol) calculated at the APFD/6–31G(d) level of theory in water using the CPCM implicit solvent model. The values in brackets correspond to the complexes, including protonated VIL.

4. Conclusions

A new, rapid, and cost-effective CE method using CD as CS has been developed for the determination of the enantiomeric purity of VIL. To identify the best system for the chiral separation of VIL, a thorough BGE and CD screening was carried out. An acetate buffer at pH 4.5 containing native α-CD as a CS proved to be the most adequate separation medium.

An experimental design-based methodology was applied for method optimization, first performing screening for significant parameters by fractional factorial design, followed by an FCCD as optimization design.

The optimized method was validated according to ICH guidelines and applied for the determination of *S*-VIL in the eutomer samples.

NMR experiments indicated an inclusion complex formation between α-CD and VIL molecules in 1:1 stoichiometry. The molecular modeling shows that the *S*-enantiomer exhibits a stronger binding to the CS than its antipode, which is in accordance with the experimental migration order. Moreover, the possibility of the formation of two complex types was demonstrated, one involving the adamantane moiety of VIL and the other involving its pyrrolidine moiety in the interactions with α-CD. The use of molecular modeling techniques further emphasizes the exploration of structural symmetry and interactions in the formation of inclusion complexes.

The developed method represents a good alternative to those already reported in the literature due to its simplicity and high efficacy. The application of native α-CD as CS, along with an aqueous separation media, provides an economically and ecologically advantageous approach for the enantiomeric impurity control of VIL. The accessibility and low cost of α-CD represent a real benefit to the more expensive ionic or single isomer CD derivatives, as well as chiral chromatographic columns. This study, through its comprehensive approach, contributes to the understanding of symmetry-related aspects in chiral analysis.

Supplementary Materials: The following supporting information can be downloaded at: https://www.mdpi.com/article/10.3390/sym16010017/s1, Figure S1: ^{1}H NMR (500 MHz) spectrum of *S*,*R*-VIL 2:1 mixture with α-CD in 1:3 ratio in D2O; Figure S2: ^{13}C NMR (125 MHz, deptqsp) spectrum of *S*,*R*-VIL 2:1 mixture with α-CD in 1:3 ratio in D_2O; Table S1: Experimental plan and results obtained for the 2^{5-2} type fractional factorial design; Table S2: Experimental plan and results obtained for the FCCD.

Author Contributions: Conceptualization, L.A.P., G.H. and Z.I.S.; methodology, L.A.P., B.S.-S., T.G., B.F. and G.T.; software, B.S.-S. and B.F.; validation, G.H., Z.I.S. and G.T.; formal analysis, L.A.P.; investigation, G.H., B.S.-S., T.G. and B.F.; resources, G.H. and G.T.; data curation, L.A.P. and G.T.; writing—original draft preparation, L.A.P. and G.H.; writing—review and editing, L.A.P., G.H., Z.I.S. and T.G.; visualization, B.F. and M.K.; supervision, G.H. and G.T.; project administration, L.A.P.; funding acquisition, L.A.P. All authors have read and agreed to the published version of the manuscript.

Funding: This work was supported by a grant from the Ministry of Research, Innovation and Digitization, CNCS—UEFISCDI, project number PN-III-P1-1.1-PD-2021-0117, within PNCDI III.

Data Availability Statement: The data presented in this study are available upon request from the corresponding author.

Acknowledgments: The GITDA (Governmental Information-Technology Development Agency, Hungary) is gratefully acknowledged for allocating computing resources used in this work. Further calculations have been carried out using resources provided by the Wroclaw Centre for Networking and Supercomputing.

Conflicts of Interest: Z.I.S. was employed by the company Sz-Imfidum, Ltd., while T.G. by Servier Research Institute of Medicinal Chemistry (SRIMC) The remaining authors declare that the research was conducted in the absence of any commercial or financial relationships that could be construed as a potential conflict of interest. The funders had no role in the design of this study; in the collection, analyses, or interpretation of data; in the writing of the manuscript; or in the decision to publish the results.

Abbreviations

ANOVA—Analysis of variance; APFD—Austin–Petersson–Frisch functional with dispersion; BGE—background electrolyte; CD—cyclodextrin; CE—capillary electrophoresis; CM-β-CD—carboxymethyl-β-cyclodextrin; CS—chiral selector; DAD—diode array detector; DIMEB—heptakis(2,6-di-O-methyl)-β-cyclodextrin; DPP-4—dipeptidyl-peptidase-4; EOF—electroosmotic flow; FCCD—face-centered central composite design; 2-HE-β-CD—2-hydroxyethyl-β-cyclodextrin; 2-HP-β-CD—2-hydroxypropyl- β-cyclodextrin; HPLC—high-performance liquid chromatography; ICH—International Council of Harmonization; LOD—limit of detection; LOQ—limit of quantification; M-β-CD—methyl-β- cyclodextrin; NMR—nuclear magnetic resonance; RSD—relatice standard deviation; S-β-CD—sulfated-β-cyclodextrin; SBE-α-CD—sulfobutyl-ether-α-cyclodextrin; SBE-β-CD—sulfobutyl-ether-β-cyclodextrin; Su-β-CD—succinyl-β-cyclodextrin; TRIMEB—heptakis(2,3,6-tri-O-methyl)-β-cyclodextrin; VIL—vildagliptin.

References

1. Dowarah, J.; Singh, V.P. Anti-diabetic drugs recent approaches and advancements. *Bioorg. Med. Chem.* **2020**, *28*, 115263. [CrossRef] [PubMed]
2. Keating, G.M. Vildagliptin: A review of its Use in type 2 diabetes mellitus. *Drugs* **2014**, *74*, 587–610. [CrossRef] [PubMed]
3. Henness, S.; Keam, S.J. Vildagliptin. *Drugs* **2006**, *66*, 1989–2001. [CrossRef] [PubMed]
4. Bernardo-Bermejo, S.; Sánchez-López, E.; Castro-Puyana, M.; Marina, M.L. Chiral capillary electrophoresis. *TrAC Trends Anal. Chem.* **2020**, *124*, 115807. [CrossRef]
5. Orlandini, S.; Hancu, G.; Szabó, Z.I.; Modroiu, A.; Papp, L.A.; Gotti, R.; Furlanetto, S. New Trends in the Quality Control of Enantiomeric Drugs: Quality by Design-Compliant Development of Chiral Capillary Electrophoresis Methods. *Molecules* **2022**, *27*, 7058. [CrossRef] [PubMed]
6. Scriba, G.K.E.; Jáč, P. Cyclodextrins as chiral selectors in capillary electrophoresis enantioseparations. In *Methods in Molecular Biology*; Humana Press Inc.: Totowa, NJ, USA, 2019; Volume 1985, pp. 39–356. [CrossRef]

7. Peluso, P.; Chankvetadze, B. Native and substituted cyclodextrins as chiral selectors for capillary electrophoresis enantioseparations: Structures, features, application, and molecular modeling. *Electrophoresis* **2021**, *42*, 1676–1708. [CrossRef] [PubMed]
8. Scriba, G.K.E. Chiral recognition in separation sciences. Part I: Polysaccharide and cyclodextrin selectors. *TrAC—Trends Anal. Chem.* **2019**, *120*, 115639. [CrossRef]
9. Chankvetadze, B.; Scriba, G.K.E. Cyclodextrins as chiral selectors in capillary electrophoresis: Recent trends in mechanistic studies. *TrAC—Trends Anal. Chem.* **2023**, *160*, 116987. [CrossRef]
10. Chankvetadze, L.; Servais, A.C.; Fillet, M.; Salgado, A.; Crommen, J.; Chankvetadze, B. Comparative enantioseparation of talinolol in aqueous and non-aqueous capillary electrophoresis and study of related selector-selectand interactions by nuclear magnetic resonance spectroscopy. *J. Chromatogr. A* **2012**, *1267*, 206–216. [CrossRef] [PubMed]
11. Gogolashvili, A.; Chankvetadze, L.; Takaishvili, N.; Salgado, A.; Chankvetadze, B. Separation of terbutaline enantiomers in capillary electrophoresis with neutral cyclodextrin-type chiral selectors and investigation of the structure of selector-selectand complexes using nuclear magnetic resonance spectroscopy. *Electrophoresis* **2020**, *41*, 1023–1030. [CrossRef] [PubMed]
12. Kazsoki, A.; Fejos, I.; Sohajda, T.; Zhou, W.; Hu, W.; Szente, L.; Béni, S. Development and validation of a cyclodextrin-modified capillary electrophoresis method for the enantiomeric separation of vildagliptin enantiomers. *Electrophoresis* **2016**, *37*, 1318–1325. [CrossRef] [PubMed]
13. Srinivas, C.; Qureshi, H.K.; Veeresham, C.; Srinivas, C.; Qureshi, H.K.; Veeresham, C. Validated Chiral Ultra Fast Liquid Chromatographic Method for Quantitative Analysis of Enantiomeric Vildagliptin. *Am. J. Anal. Chem.* **2021**, *12*, 429–439.
14. Papp, L.A.; Hancu, G.; Szabó, Z.I. Simultaneous determination of enantiomeric and organic impurities of vildagliptin on a cellulose tris(3-chloro-4-methylphenylcarbamate) column under revered-phase conditions. *J. Pharm. Biomed. Anal.* **2023**, *234*, 115495. [CrossRef] [PubMed]
15. Jorgensen, W.L.; Maxwell, D.S.; Tirado-Rives, J. Development and testing of the OPLS all-atom force field on conformational energetics and properties of organic liquids. *J. Am. Chem. Soc.* **1996**, *118*, 11225–11236. [CrossRef]
16. Trott, O.; Olson, A.J. AutoDock Vina: Improving the speed and accuracy of docking with a new scoring function, efficient optimization, and multithreading. *J. Comput. Chem.* **2009**, *31*, 455–461. [CrossRef] [PubMed]
17. Stewart, J.J.P. Optimization of parameters for semiempirical methods V: Modification of NDDO approximations and application to 70 elements. *J. Mol. Model.* **2007**, *13*, 1173–1213. [CrossRef] [PubMed]
18. Austin, A.; Petersson, G.A.; Frisch, M.J.; Dobek, F.J.; Scalmani, G.; Throssell, K. A density functional with spherical atom dispersion terms. *J. Chem. Theory Comput.* **2012**, *8*, 4989–5007. [CrossRef] [PubMed]
19. Frisch, M.J.; Trucks, G.W.; Schlegel, H.B.; Scuseria, G.E.; Robb, M.A.; Cheeseman, J.R.; Scalmani, G.; Barone, V.; Petersson, G.A.; Nakatsuji, H.; et al. *Gaussian 16, Revision, C.01*; Gaussian, Inc.: Wallingford, CT, USA, 2019.
20. Barone, V.; Cossi, M. Quantum calculation of molecular energies and energy gradients in solution by a conductor solvent model. *J. Phys. Chem. A* **1998**, *102*, 1995–2001. [CrossRef]
21. Cossi, M.; Rega, N.; Scalmani, G.; Barone, V. Energies, structures, and electronic properties of molecules in solution with the C-PCM solvation model. *J. Comput. Chem.* **2003**, *24*, 669–681. [CrossRef] [PubMed]
22. Chankvetadze, B. Contemporary theory of enantioseparations in capillary electrophoresis. *J. Chromatogr. A* **2018**, *1567*, 2–25. [CrossRef] [PubMed]